Accepted Manuscript

Application of multivariate statistical analyses to *Itrax*^{TM} core scanner data for the identification of deep-marine sedimentary facies: A case study in the Galician Continental Margin

A.E. López Pérez, D. Rey, V. Martins, M. Plaza-Morlote, B. Rubio

PII: S1040-6182(18)30103-4

DOI: 10.1016/j.quaint.2018.06.035

Reference: JQI 7495

To appear in: *Quaternary International*

Received Date: 31 January 2018

Revised Date: 4 May 2018

Accepted Date: 21 June 2018

Please cite this article as: López Pérez, A.E., Rey, D., Martins, V., Plaza-Morlote, M., Rubio, B., Application of multivariate statistical analyses to *Itrax*^{TM} core scanner data for the identification of deep-marine sedimentary facies: A case study in the Galician Continental Margin, *Quaternary International* (2018), doi: 10.1016/j.quaint.2018.06.035.

Application of multivariate statistical analyses to *Itrax*^{TM} core scanner data for the identification of deep-marine sedimentary facies: a case study in the Galician Continental Margin.

A.E. López Pérez[1], D. Rey[1], V. Martins[2,3], M. Plaza-Morlote[1], B. Rubio[1]*

1. GEOMA, Dpto. Geociencias Marinas y O.T., Universidade de Vigo, 36310, Vigo, Spain.
2. Universidade do Estado do Rio de Janeiro, Av. São Francisco Xavier, 524, Maracanã. CEP 20550-013, Rio de Janeiro, RJ, Brazil.
3. GeoBioTec, Dpto. Geociências, Universidade de Aveiro, Campus de Santiago, 3810-193 Aveiro, Portugal

*Corresponding author

Abstract

The validity and usefulness of multivariate statistical tools for the facies characterization in deep-marine environments have been applied on the geochemical, sedimentological and magnetic data from a piston core extracted from the Transitional Zone in the Galician Continental Margin. The combination of geochemical profiles of Fe, Mn, Ti, Ba and Ca and magnetic susceptibility (MS) obtained using the *Itrax*^{TM} Core Scanner at the University of Vigo, together with the grain-size, grey level and R (red) G (green) B (blue) colour analyses have allowed characterizing and classifying the sediments of the core PC13-3 using SPSS package v. 23. Cluster Analysis (CA) displays, in the first level of the hierarchy, two major groups that correspond with clay-silt and sand facies. In a second level, it is possible to observe six subfacies that match *de visu* preliminary classification and allowed us to complete and improve the characterization and the facies limits in the whole core. Discriminant Analysis (DA) confirmed the validity of the cluster analyses and enhanced the results of the classification. The Principal Component Analysis (PCA) shows four principal components: coarse lithogenic fraction (PC1), fine lithogenic fraction (PC2), high density fraction (PC3) and biogenic fraction (PC4). These results are in concordance with the Pearson correlation coefficient and the SEM observations. In general terms, the results confirm the utility of the multivariate statistical methods applied on high resolution geochemical and magnetic data acquired with *Itrax*^{TM} corer scanner, as a quick and complementary tool in sedimentary facies analysis and description in deep marine environments.

Keywords: *Galicia Continental Margin, Sedimentology, facies analysis, multivariate statistical analysis, Itrax*^{TM} *Core Scanner*

Introduction

In general, sedimentological facies classification is based on visual description/interpretation and qualitative analysis of the sediment core. Currently, this methodology is still widely used and provides good results. A large number of works show examples of this, such as Lamourou et al., (2017) who identified six sedimentary facies based on microscopic observations in Quaternary deposits in the Gabes Gulf located in the southeast of Tunisia coast. However, there is a tendency to quantify or systematize the classification of facies employing multivariate statistical analyses such as Cluster Analysis (CA), Discriminant Analysis (DA) or/and Principal Component Analysis (PCA). Barbera et al., (2009) used PCA and discriminant function analyses on mineralogical (x-ray diffraction) and geochemical (x-ray fluorescence) data to demonstrate provenance and continental sedimentary history in mudrocks. Rey et al., (2008) characterized five magnetochemical facies to determine different sedimentary marine environments using CA on geochemical and magnetic data acquired with XRF-CORTEX (core scanner Texel) and cryogenic magnetometer. Margalef et al., (2013) performed facies analysis using PCA on Fe, Ti and Ca data measured with *Itrax* ^{TM} corer scanner, along with other discrete analysis (TC, TN and δ13C) and macrofossil analysis in marine sediments located at the central South Pacific Ocean. Baumgarten et al., (2014) carried out CA on XRF data got with an Avaatech XRF core Scanner III to define lacustrine sediment characteristics. Flood et al., (2015; 2018) used grain size, mineralogy and geochemistry data (obtained through *Itrax* ^{TM} corer scanner) to define grain size variability, provenance and depositional environments from a fine tidal estuary sediments using a multivariate statistical methodology based on PCA and CA. Recently, Nugroho et al., (2017) used CA and DA to characterize marine sedimentary facies and depositional environments using grain size statistical parameters and compositional data.

Other studies evidence the utility of high-resolution data obtained with the *Itrax*^{TM} core scanner to identify facies and microfacies in varved lakes core sediments, such as demonstrated Dulski et al., (2015).

Despite these interesting works, the use of multivariate statistical methods in the facies analysis and depositional environment characterization is very scarce when compared with other fields such as environmental pollution and quality control in sediments (Rubio et al., 2000; Martins et al., 2016) and groundwaters (Tlili-Zrelli et al., 2013).

The previous studies have demonstrated the advantage of using multivariate statistical analysis (CA, DA and PCA) combining different geochemical, magnetic and grain-size data against *de visu* descriptions to classify facies in deep-marine environments with statistical confidence. CA allows a quick classification of the samples by grouping samples with similar characteristics, while the DA provides a statistical assessment and refinement of the CA grouping. At the same time, PCA allows defining new variables or components related to the sedimentological and geochemical properties of the sediment.

This paper will explore how this approach can give greater consistency, reliability, sensitivity and objectivity to facies classification than the more common *de visu* procedure, particularly when it is based on a large and diverse number of variables (i.e. geochemical, sedimentological and magnetic). The main advantage of these statistical methods lies in the fact that these analyses constitute a fast exploratory method, supported by statistical parameters that improve the facies distinction with very subtle changes. *De visu* classification is very dependent of the observer´s experience and could lead to errors in relatively homogeneous sedimentary records, with subtle changes in grain-size and variations in magnetic and/or geochemical properties. This study, unlike to the previous referenced works, uses magnetic susceptibility data (1 cm) and raw high-resolution geochemical, colour and grey level data (1 mm) (smoothed to each cm to improve results) obtained with the Itrax^{Tm} corer scanner. This high-resolution data allow a better discrimination of the facies classification, even at millimeter scale. The combination of these high-resolution data with the traditional lower resolution grain size data supposes an advantage in facies description because let detect subfacies and subtle limits along the whole core, very difficult to detect in the *de visu* classification. Selecting the appropriate variables dataset allows discriminating between sedimentological and provenance processes in deep marine environments, mainly between pelagic and hemipelagic processes.

Our approach allows differentiating a high number of facies in comparison with the previous *de visu* procedure based on a high-resolution dataset obtaining by XRF-scanner and supported by statistical analyses. This fact is representing a considerable advantage with the classical visual description facies classification commonly used and constitutes a refined approach of the using of multivariate statistical methods in the facies classification field.

Materials and methods

This work is based on a 4.28 m long PC13-3 piston core taken at 1,688 m depth in the Transitional Zone (TZ) province (Ercilla et al., 2008; 2011; Vázquez et al., 2008) in the Galicia Continental Margin. The core was collected during the "Burato 4240" oceanographic cruise on board the R/V Sarmiento de Gamboa in September 2010 (latitude 42°43'04.01''N, longitude 11°09'19.43''W) (Fig. 1). The TZ is characterized by three giant pockmark structures that have been related to large-scale fluid escapes. PC13-3 is extracted at NW of one of these structures, known as *Gran Burato*, which has a circular morphology of 4 km in diameter, with maximum depths of 375 m, and is characterized by high slopes. The facies classification of the PC13-3 core will allow knowing the affection in the local sedimentation of the fluid escape processes.

Optical and radiographical images were obtained with the *Itrax*^{TM} Core Scanner at the University of Vigo, as well as geochemical and magnetic susceptibility data, using the Mo-tube with a voltage of 30 kV and an exposure time of 20 seconds. The high-resolution XRF geochemical raw data (1mm step size) were smoothed using a 1 cm running mean to validate and improve their reliability (Rodríguez-Germade et al., 2013). Radiographic data were exported to grey-scale data files with the Redicore software of the core scanner. Colour data were obtained in RGB values from the optical images obtained with the *Itrax*^{TM} core scanner.

Grain-size distributions were determined from discrete samples collected every 4 cm using a laser diffraction particle size analyzer Coulter LS230 (Beckman) at the *Department d´Estratigrafia, Paleontologia I Geociències Marines de la Universitat de Barcelona.*

The petrology of the core was studied employing a JEOL JSM-6700f Scanning Electron Microscope (SEM), operating in back-scattering mode (BS), located at the C.A.C.T.I. of the University of Vigo.

The statistical analyses (CA, DA and PCA) were carried out using the SPSS package v.23 for a total of 15 variables analyzed in 106 samples (1590 data points).

Results and discussions

1. General sediment properties

Table 1 summarizes descriptive statistical values for the grain-size, geochemical and magnetic sediment properties obtained by the SPSS v.23 software. In general terms, PC13-3 core contents an average sand, silt and clay percentage of 45.19 ± 32.62 %, 26.40 ± 11.68 %, and 28.42 ±

23.61 %, respectively. The mean grain size is 88.39 ± 69.28 μm (φ = 3.50 ± 3.85). Regarding the sorting, this parameter shows a value of 66.50 ± 43.28 μm (3.91 ± 4.53 φ), so the general description of the core corresponds with very fine sand very poorly sorting. The statistic results of RGB components present mean values of 231.44 ± 13.92 for the red, 209.29 ± 23.56 for the green and 171.20 ± 39.91 for the blue, corresponding with sienna tonalities.

Regarding the geochemical results, elements such as Fe, Ti, Ba and Mn show mean values of 17,581.06 ± 12,549.91 peak areas (p.a.), 379.95 ± 347.47 p.a., 43.71 ± 23.55 p.a. and 223.86 ± 157.58 p.a. respectively, are being the iron the metal element that presents more variability between maximum and minimum values. Ca shows a mean value of 162,539.43 ± 39,283.20 p.a., as well as the highest difference between the maximum and minimum value. Respect to the MS the mean value obtained is 6.29 10^{-5} ± 7.59 SI and also presents a high variability between samples (range varied from 0.20 10^{-5} - 48.40 10^{-5} SI). Finally, the Grey Level (GL), a parameter related to the density, shows mean value of 33,555.91 ± 110.21.

Pearson correlation matrix (Table 2) show most variables are well correlated ($p < 0.01$). Clay and silt show a noticeable positive correlation ($r = 0.850$) and these both variables present negative correlation with Sand, Mean Grain Size (MGS) and sorting ($r = -0.844$, $r = -0.920$ and $r = -0.891$ for the clay and $r = -0.665$, $r = -0.728$ and $r = -0.685$ for the silt respectively). Sand shows a positive correlation between MGS and Sorting ($r = 0.952$ and $r = 0.948$ respectively). These correlations could indicate a large variability of the grain-size in the sedimentary record, being sand the most abundant size in the core (high positive correlation between sand and MGS). Moreover high positive correlation is noticeable between Fe *vs*. Ti ($r = 0.938$ and $p<0.01$) and is remarkable the positive correlation between MS *vs*, Fe, Ti, Ba, and Mn. This could be related to lithogenic components with high metallic elements content. Regarding Ca, this element shows positive correlation with RGB variables and a negative correlation with others metallic elements (Fe, Ti, Ba, and Mn) and MS, that could be associated to biogenic components with high Ca and low metallic elements.

2. Statistical Analysis

2.1. Statistical Analysis applications

Cluster Analysis (CA) is a statistical exploration tool that allows to group samples by its degree of similarity. This analysis is widely used to study the pattern of distribution and provenance of sediments in depositional environments based on grain-size, geochemical and/or magnetic data (Kim et al., 2013; Kolesnik et al., 2017). Discriminant Analysis (DA) allows obtaining a discriminant function based on linear combinations of the variables and allows predicting and differentiating the ones, which belong to a particular group of the samples. Principal Component Analysis (PCA) reduces the dimensionality of the dataset by linear compilations of correlated variables called Principal Components (PCs). DA and PCA are typically used in assessment pollution or in the distribution of metals elements in marine sediments (Rubio et al., 2000; Farmaki et al., 2014), but very rarely for facies classification.

2.2. Cluster analyses

Cluster analysis (CA) was run in Q mode using the unweighted pair group method with arithmetic mean (UPGMA method) and the Euclidean squared distance as the similarity coefficient. Previously, with the objective of testing the uniformity and normality of the data, Kolmogorov-Smirnov and Saphiro-Wilk tests were performed on all variables, confirming the non-normal distribution of the variables except for the variables of silt, MS and green colour. All data were normalized using a logarithmic transformation to obtain better results and avoid the effect of differences in magnitude and variance of the data (Rubio et al. 2001).

Fig. 2 shows the obtained dendrogram, where two main clusters (CLA and CLB) in the first level of the hierarchical dendrogram and six subclusters (S1 to S6) in the second hierarchy level are identified. CLA comprises all samples with sand content below of 17 % and CLB samples with sand percentage higher than 17 %. CLA is divided into two subfacies, S1 and S2. Cluster S1 groups samples with sand percentage between 0 and 2% and S2 clusters samples with sand percentage between 4 % and 17 %. CLB group includes subclusters CL1 and CL2. CL1 contain two subfacies depending on the sand content: S3 enclose samples with sand percentage between 17 % and 66 % and S4 groups samples with sand percentage higher than 69 %. Both subfacies do not include samples with high content of metallic elements, and high values of MS. CL2 includes S5 and S6 subfacies, which grouped samples with higher content in Fe, Ti, and MS in the whole core. S5 shows lower values of Fe, Ti and MS (19,800.91 p.a., 435.86 p.a. and 12.41 10^{-5} SI respectively) than S6, which displays the highest values for Fe, Ti and MS parameters (50,959.20 p.a., 1,303.41 p.a. and 17.02 10^{-5} SI respectively).

2.3. Discriminant Analysis

DA was performed by the stepwise method to obtain the percentage of correct prediction to validate statistically the different groups obtained by cluster analysis. Prior to the DA, Box´s M Test was carried out to check the validity of the hypothesis of equal covariance. Results ($p<0.05$) reject the null hypothesis of equality of matrices of covariance, so DA was performed obtained a percentage of 98.1 % of correct predictions of samples classified by CA (Table 3 and Fig. 3).

Only two samples (47 and 60) show a different classification in DA, which differs from the CA results. Sample 47 was classified by CA in S4 meanwhile the DA predicted that it pertains to S5 in the highest group classification and S4 in the second highest group. The probability of pertaining to the predicted highest group has a value of 0.576 and shows a Mahalanobis distance of 8.976. On the other hand, the probability of correct classification in the second highest group has a value of 0.361 and shows a Mahalanobis distance value (9.910) very similar in comparison to the distance indicator in the highest group. Additionally, sample 47 present a grain-size, geochemical and magnetic values situated in CA in the high limit of S4 close to the low limit of S5. Regarding the sample 60, it was clustered in S3 using CA meanwhile DA grouped it in S2 in the highest group and S3 in the second highest group classification. The value of probability of belong to the assigned highest group is 0.997, and its Mahalanobis distance from the group centroid of S2 is 10.712. Otherwise, the probability to pertain to the second predicted highest group is 0.03, and its Mahalanobis distance (22.500) is much higher than the first predicted group distance. Moreover, this sample has a percentage of sand of 17.18 %, being the grain-size lower limit of S3 suggested by CA. These grain-size values are more similar to the samples grouped in S2 (mean sand percentage of 10.13 %) than samples in S3 (mean sand percentage of 53.08 %).

Taking into account all these considerations from DA (probabilities and Mahalanobis distances) and the geochemical, magnetic and grain-size subcluster limits values, we determinate that sample 47 was correctly classified in S4 using CA meanwhile sample 60 was not correctly classified in S3. This sample pertains to S2 as demonstrated the statistical results obtained by DA ($p = 0.997$ and Mahalanobis distance = 10.712). Moreover, the low value of Wilks's lambda (0.001), along with the high value of chi-square (1331.03), allowed us to ensure the validity of the groupings of facies classification ($p < 0.0001$). Thus we can determine the useful and complementarity of DA in facies classification to verify and improve CA results, due to this analysis allow obtaining statistical parameters that validate the classification.

Table 4 contains the correlations of the variables with the five first discriminant functions and indicates the variables selected and used in the discriminant analysis (sand, sorting, Fe, Mn, clay, SM and silt). This suggests that these variables have more weight in the dataset than the rest of variables.

2.4. Principal Component Analysis

Principal component analysis (PCA) was performed on all data to obtain principal components that allow describing and characterizing the sediments and geochemical properties of the core. For this purpose normalized and standardize data using logarithmic transformations were again applied without rotation of the matrix. Moreover, the MGS was removed from the matrix owing to it is related to the grain size and show high correlation with the sand.

Four components have been extracted, explaining the 87.07% of the total variance (Table 5).The PC1 groups the variables of sand, sorting, Fe, Ti, Ba Mn and MS, which shows high correlation. Moreover, it is remarkable their negative correlation with clay, Ca and RGB colour variables. This component represents 48.78 % of the total variance of data. PC2 explains 26.44 % and groups silt, clay and metal transition variables and show negative significant correlation of GL. PC3 represents 6.87 % of the variance of all data and only shows significant negative correlation of GL parameter. Finally, PC4 represents 4.98% of the total variance and shows significant positive Ca correlation. Results of the PCA are in concordance with the Pearson correlation matrix.

PC1 was interpreted as a coarse lithogenic component rich in metal transition elements and high MS. Meanwhile, variables groups in PC2 allowed us to describe this association as fine lithogenic component. PC3 was identified as a high-density component related to the fine lithogenic component. Both, PC2 and PC3 show a significant negative correlation of GL. PC2 also shows a significant positive correlation with clay and silt. This means that samples with high content in fine-grain sediments have low values of GL, an indicative of high density, because the porosity in clay and silt fraction is lower than in sands. PC4 was described as biogenic component.

The interpretation of these four components can be observed by SEM (Fig. 4). The Fig. 4a and Fig 4b shows well-preserved foraminifera sands with terrigenous components of different sizes and Fig. 4c and Fig. 4d shows magnetite and ilmenomagnetite respectively. These terrigenous components constitute the coarse lithogenic rich in transition elements (PC1) and the fine lithogenic component (PC2) related to the high density component (PC3). Finally, Fig. 4e shows a small proportion of well-preserved foraminifera in a coccolithophoridae matrix (Fig. 4f). This matrix, along with the well-preserved foraminifera along the whole core, defines the biogenic component (PC4).

3. Sediment properties of subfacies classification

Fig. 5. displays the facies classification obtained after CA and DA application (Fig. 5a). This figure compares the previous visual description of the core (Fig. 5b) following by the photography (Fig. 5c), radiography (Fig. 5d) and grain-size data distribution of the core (Fig. 5e). Note that the limits between the different facies and the recognition of the high magnetic susceptibility facies along the core have significantly improved. Taking into account the new facies classification for the PC13-3, Table 6 shows the average values for the different variables for each subfacies.

Subfacies S1 presents average sand, silt and clay percentages of 0.25 %, 35.85 % and 63.89 respectively and mean values of Fe, Ti, Ca and MS of 12,891.33 p.a., 213.88 p.a., 166,495.64 p.a. and 2.63 10^{-5} SI respectively. Volumetrically it represents 8.04 % of the core. Meanwhile, S2 represents volumetrically 26.29 % of the core and presents sand, silt and clay content of 10.13 %, 46.72 % and 43.15 % for each variable and Fe, Ti, Ca and MS average of 13,367.84 p.a., 279.69 p.a., 178,198.01 p.a. and 4.74 10^{-5} SI respectively. S3 represents 16.65 % of the core and displays an average mean percentage of sand, silt, and clay of 53.08 %, 24.94 %, and 21.98 % respectively. Moreover Fe, Ti, Ca and MS show an average of 11,835.36 p.a., 252.76 p.a., 189,383.77 p.a. and 3.01 10^{-5} respectively. Regarding S4 represents volumetrically 19.69 % of the whole core and shows mean values of sand, silt, and clay of 80.97 %, 13.27 %, and 5.77 % respectively. Also, it shows an average value for Fe, Ti, Ca and MS of 11,920.71 p.a., 242.37 p.a., 185,141.13 p.a. and 2.90 10^{-5} SI respectively. S5, that represent volumetrically the 19.21 %, contents percentages of sand, silt and clay of 70.15 %, 19.37 % and 10.48 % respectively and Fe, Ti, Ca and MS values of 19,800.91 p.a., 435.86 p.a., 129,951.01 p.a. and 12.41 10^{-5} SI for each variable mentioned. Finally, S6 shows a mean percentage of sand, silt, and clay of 50.29 %, 30.24 % and 19.47 % respectively and represents 10.12 % of the whole core. Regarding Fe, Ti, Ca and MS parameters, S6 displays values of 50,959.20 p.a., 1,303.51 p.a., 115,241.88 p.a. and 17.02 10^{-5} SI respectively.

4. Sedimentological significance of the CA, DA and PCA results

A precise combination of the variables in the matrix dataset, and the use of limits obtained by the statistical analyses, allow interpret processes (pelagic and hemipelagic) and provenance of the sediment record (detrital and biogenic), considering confidence intervals for CA, DA and PCA, combined with Pearson correlation and SEM observations. The variables dominant in hemipelagic detrital facies are Fe, Ti, and MS, in pelagic biogenic facies is mainly Ca.

S1 and S2 clustering in CLA by CA, classified samples corresponding to a clay-silt grain size that show high Ca content, low Fe and Ti content and low-susceptibility. These samples defined as Ca-rich low-susceptibility silt-clay facies (*Car-lok silt-clay facies*) and described as silt-clay pelagite. S3 and S4 included in CL1 of CLB, content foraminifera-sand samples characterized by high Ca content, low Fe and Ti content and low-susceptibility. These samples named as the Ca-rich low-susceptibility sand facies (*Car-lok sand facies*) and interpreted as sand pelagite. S5 and S6 grouping in CL2 of CLB, display foraminifera-sand samples with the highest content of Fe, Ti and most upper MS values. These samples classified as Fe-Ti high susceptibility sand facies (*Fe-Ti sand facies*) and described as hemipelagic magnetic layers interbedded in the pelagic sediment that could be related to IRDs layers deposited during the Heinrich Events. CA, DA and PCA allow to identify three different clay-silt and sand facies that correspond to pelagic and hemipelagic sediments.

Conclusions

The combination of high-resolution *Itrax*^{TM} core scanning determination of Fe, Ti, Ca, Mn, Ba and magnetic susceptibility profiles with colour RGB, grey line data, detailed grain-size and other grain-size parameters (MGS and sorting) in the same data set, have allowed to characterize and to classify the sediments of the PC13-3 core using multivariate statistical method through the SPSS package v.23. Descriptive statistics results, combined with the SEM observations, allowed us to describe the sediment of the study core as a very fine foraminifera-sand very poor sorting. CA shows two major facies (CLA and CLB) and six subfacies that correspond with the hemipelagite and pelagite in a previous visual classification. CA results allowed us to complete and improve the characterization and the limits of the facies and subfacies of the core, allowing establishing better limits for subtle differences. DA allowed statistically validates the clusters obtained and improved their results. DA results showed that, overall, more than 98.1% of the samples grouped by the CA are properly classified. Moreover, the low value of lambda Wilks statistic (0.001), along with the high value of chi-square (1331.03) allowed validating the facies classification made by CA ($p < 0.0001$). Thus, the combination of CA and DA constitute a complementary multivariate statistical tool in the field of facies classification because establishes a robust statistical methodology to determinate the facies classification and confirm their validity. The combination of both analyses allows us to obtain a statistical value by DA that provides a reliance statistical weight to the CA classification, confirming the utility and confidence of these kinds of tools in marine facies classification. Moreover, PCA shows four principal components, described as coarse lithogenic fraction (PC1), fine lithogenic fraction (PC2), high density fraction (PC3) and biogenic fraction (PC4). These results are in concordance with the Pearson correlation coefficient and the SEM observations. We can conclude that multivariate statistical analyses (CA, DA, and PCA) constitute a useful and fast complementary tool in facies classification applied to *Itrax* ^{TM} core scanner data that let improves the visual facies characterization in deep-marine environments.

Acknowledgements

This work was funded by the Gran Burato 2010 and 2011 convenia between the University of Vigo, CSIC, and Xunta de Galicia, and the MINECO Project CGL2008-034774-E. We want to thank the captains and crew of the R/V Sarmiento de Gamboa, the UTM technical support and the GB4240 and GB2011 cruise participants.

References

Barbera, G., Lo Giudice, A., Mazzoleni, P., Pappalardo, A., 2009. Combined statistical and petrological analysis of provenance and diagenetic history of mudrocks: Application to Alpine Tethydes shales (Sicily, Italy). Sedimentary Geology 213, 27–40. doi:10.1016/j.sedgeo.2008.11.002

Baumgarten, H., Wonik, T., Kwiecien, O., 2014. Facies characterization based on physical properties from downhole logging for the sediment record of Lake Van, Turkey. Quaternary Science Reviews 104, 85–96. doi:10.1016/j.quascirev.2014.03.016

Dulski, P., Brauer, A., Mangili, C., 2015. Combined µ-XRF and Microfacies Techniques for Lake Sediment Analyses. In: Micro-XRF Studies of Sediment Cores, Developments in Paleoenvironmental Research. Springer, Dordrecht, pp. 325–349. doi:10.1007/978-94-017-9849-5_12

Ercilla, G., García-Gil, S., Estrada, F., Gràcia, E., Vizcaino, A., Váquez, J.T., Díaz, S., Vilas, F., Casas, D., Alonso, B., Dañobeitia, J., Farran, M., 2008. High-resolution seismic stratigraphy of the Galicia Bank Region and neighbouring abyssal plains (NW Iberian continental margin). Marine Geology 249, 108–127. doi:10.1016/j.margeo.2007.09.009

Ercilla, G., Casas, D., Vázquez, J.T., Iglesias, J., Somoza, L., Juan, C., Medialdea, T., León, R., Estrada, F., García-Gil, S., Farran, M. l., Bohoyo, F., García, M., Maestro, A., 2011. Imaging the recent sediment dynamics of the Galicia Bank region (Atlantic, NW Iberian Peninsula). Marine Geophysical Research 32, 99–126. doi:10.1007/s11001-011-9129-x

Farmaki, E.G., Thomaidis, N.S., Pasias, I.N., Baulard, C., Papaharisis, L., Efstathiou, C.E., 2014. Environmental impact of intensive aquaculture: Investigation on the accumulation of metals and nutrients in marine sediments of Greece. Science of The Total Environment 485–486, 554–562. doi:10.1016/j.scitotenv.2014.03.125

Flood, R.P., Orford, J.D., McKinley, J.M., Roberson, S., 2015. Effective grain size distribution analysis for interpretation of tidal–deltaic facies: West Bengal Sundarbans. Sedimentary Geology 318, 58–74. doi:10.1016/j.sedgeo.2014.12.007

Flood, R.P., Barr, I.D., Weltje, G.J., Roberson, S., Russell, M.I., Meneely, J., Orford, J.D., 2018. Provenance and depositional variability of the Thin Mud Facies in the lower Ganges-Brahmaputra delta, West Bengal Sundarbans, India. Marine Geology 395, 198–218. doi:10.1016/j.margeo.2017.09.001

Kim, W., Doh, S.-J., Yu, Y., Lee, Y.I., 2013. Magnetic evaluation of sediment provenance in the northern East China Sea using fuzzy c-means cluster analysis. Marine Geology 337, 9–19. doi:10.1016/j.margeo.2013.01.001

Kolesnik, A.N., Astakhov, A.S., Kolesnik, O.N., 2017. Recent deposition environments in the Chukchi Sea and adjacent areas of the Arctic Ocean: Evidence from Q-cluster analysis of sediment compositions and grain sizes. Russian Geology and Geophysics 58, 1468–1477. doi:10.1016/j.rgg.2017.11.011

Lamourou, A., Touir, J., Fagel, N., 2017. Reconstructing the Holocene depositional environments along the northern coast of Sfax (Tunisia): Mineralogical and sedimentological approaches. Journal of African Earth Sciences 129, 713–727. doi:10.1016/j.jafrearsci.2017.01.031

Margalef, O., Cañellas-Boltà, N., Pla-Rabes, S., Giralt, S., Pueyo, J.J., Joosten, H., Rull, V., Buchaca, T., Hernández, A., Valero-Garcés, B.L., Moreno, A., Sáez, A., 2013. A 70,000 year multiproxy record of climatic and environmental change from Rano Aroi peatland (Easter Island). Global and Planetary Change 108, 72–84. doi:10.1016/j.gloplacha.2013.05.016

Martins, M.V.A., Helali, M.A., Zaaboub, N., Boukef-BenOmrane, I., Frontalini, F., Reis, D., Portela, H., Clemente, I.M.M.M., Nogueira, L., Pereira, E., Miranda, P., El Bour, M., Aleya, L., 2016. Organic matter quantity and quality, metals availability and foraminiferal assemblages as environmental proxy applied to the Bizerte Lagoon (Tunisia). Marine Pollution Bulletin 105, 161–179. doi:10.1016/j.marpolbul.2016.02.032

Nugroho, S.H., Putra, P.S., Yulianto, E., Noeradi, D., 2017. Multivariate statistical analysis for characterization of sedimentary facies of Tarakan sub-basin, North Kalimantan. Marine Georesources & Geotechnology 1–11. doi:10.1080/1064119X.2017.1399178

Rey, D., Rubio, B., Mohamed, K., Vilas, F., Alonso, B., Ercilla, G., Rivas, T., 2008. Detrital and early diagenetic processes in Late Pleistocene and Holocene sediments from the SW Galicia Bank inferred from high-resolution enviromagnetic and geochemical records. Marine Geology, Geological characterization of the Galicia Bank Region (Atlantic Ocean, NW Iberia) 249, 64–92. doi:10.1016/j.margeo.2007.09.013

Rodríguez-Germade, I., Rubio, B., Rey, D., Vilas, F., Martins, V., Rocha, F., 2013. Evaluation of data processing techniques for marine sediments analyzed with an Itrax Core Scanner. Geogaceta 53, 85–87.

Rubio, B., Nombela, M.A., Vilas, F., 2000. Geochemistry of major and trace elements in sediments of the Ria De Vigo (NW Spain): an assessment of metal pollution. Marine pollution bulletin 40, 968–980.

Tlili-Zrelli, B., Azaza, F. hamzaoui-, Gueddari, M., Bouhlila, R., 2013. Geochemistry and quality assessment of groundwater using graphical and multivariate statistical methods. A case study: Grombalia phreatic aquifer (Northeastern Tunisia). Arabian Journal of Geosciences 6, 3545–3561. doi:10.1007/s12517-012-0617-3

Vázquez, J.T., Medialdea, T., Ercilla, G., Somoza, L., Estrada, F., Fernández Puga, M.C., Gallart, J., Gràcia, E., Maestro, A., Sayago, M., 2008. Cenozoic deformational structures on the Galicia Bank Region (NW Iberian continental margin). Marine Geology 249, 128–149. doi:10.1016/j.margeo.2007.09.014

Caption to Figures

Fig. 1. Bathymetric map of the Galicia continental margin with the PC13-3 core location and the four main morphostructural provinces in the study area: Deep Galicia Margin (DGM), Galicia Bank (GB), Transitional Zone (TZ) and the Galicia Interior Basin (GIB).

Fig. 2. Dendrogram obtained using UPGMA method and the Euclidean squared distance as the similarity coefficient. A total of 106 samples were used in CA.

Fig. 3. Plot of the canonical discriminant functions obtained by DA.

Fig. 4. SEM micrographs obtained at different depths of the PC13-3 core. a) Fe-Ti sand facies at 35 cm composed by foraminifera and terrigenous components. b) Fe-Ti sand facies at 54 cm composed by foraminifera and terrigenous components. c) Magnetite located at 105 cm in Fe-Ti sand facies. d) Ilmenomagnetite located in Fe-Ti sand facies at 105 cm. e) Car-lok silt-clay facies at 400 cm f) Car-lok silt-clay facies at 400 cm with optical magnifying where it is possible to recognize the coccolithophoridae matrix.

Fig. 5. a) Facies description obtained using multivariate statistical methods b) previous visual facies description c) optical and d) radiographical images obtained with the Itrax^{TM} Corer scanner, followed by a grain size distribution (e). Note the improvement on the facies classification by using multivariate statistical methods.

Tables

Table. 1. Statistical values from the variables used for the statistical described of the PC13-3 core.

Variable	Mean	S.D.	Minimum	Maximum
Clay (%)	28.42	23.61	1.89	78.94
Silt (%)	26.40	11.68	7.82	56.20
Sand (%)	45.19	32.62	0.00	89.49
MGS (µm)	88.39	69.28	3.62	245.86
Sorting (µm)	66.50	43.28	4.88	152.83
Fe (p.a.)	17,581.06	12,549.91	6,265.55	78,318.91
Ti (p.a.)	379.95	347.47	90.82	2,161.64
Ba (p.a.)	43.71	23.55	15.09	161.55
Mn (p.a.)	223.86	157.58	66.82	950.64
Ca (p.a.)	162,539.43	39,283.20	53,594.73	227,924.18
GL	33,555.91	110.21	33,368.82	33,867.82
MS (10^{-5} SI)	6.29	7.59	0.20	48.40
Red	231.44	13.92	161.73	242.36
Green	209.29	23.56	136.45	253.09
Blue	171.20	39.91	90.00	250.00

106 samples used in the analysis. MGS= Mean Grains Size, GL = Grey Level, MS = Magnetic Susceptibility and S.D.= Standard Desviation

Table. 2. Pearson correlation matrix for the variables.

	Clay	Silt	Sand	MGS	Sorting	Fe	Ti	Ba	Mn	Ca	GL	MS	Red	Green	Blue
Clay	1.000	.850**	-.844**	-.920**	-.891**	-.071	-.185	-.127	.103	.078	-.449**	-.272**	.092	.426**	.462**
Silt		1.000	-.665**	-.728**	-.685**	.134	.061	.056	.279**	-.077	-.404**	-.042	-.068	.200*	.240*
Sand			1.000	.952**	.948**	.196*	.336**	.192*	.018	-.088	.329**	.350**	-.223*	-.437**	-.477**
MGS				1.000	.995**	.160	.296**	.167	-.074	-.062	.411**	.324**	-.155	-.466**	-.503**
Sorting					1.000	.172	.308**	.182	-.052	-.059	.380**	.331**	-.175	-.472**	-.505**
Fe						1.000	.938**	.777**	.666**	-.577**	-.024	.701**	-.768**	-.812**	-.814**
Ti							1.000	.813**	.641**	-.472**	-.009	.688**	-.728**	-.797**	-.798**
Ba								1.000	.727**	-.471**	-.225*	.538**	-.692**	-.647**	-.624**
Mn									1.000	-.527**	-.405**	.503**	-,589**	-.512**	-.487**
Ca										1.000	.150	-.521**	.636**	.662**	.637**
GL											1.000	.116	.107	-.216*	-.227*
MS												1.000	-.543**	-.726**	-.715**
Red													1.000	.739**	.709**
Green														1.000	.977**
Blue															1.000

106 samples were used for the correlation analysis. MGS= Mean Grains Size, GL = Grey Level and MS = Magnetic Susceptibility.

** $p < 0.01$
* $p < 0.05$

Table. 3. Results of correct predictions of samples classified by CA**.**

Classification results[a]

Subfacies			Predicted Group Membership						Total
			S1	S2	S3	S4	S5	S6	
Original	Count	S1	27	0	0	0	0	0	27
		S2	0	7	0	0	0	0	7
		S3	0	1	18	0	0	0	19
		S4	0	0	0	20	1	0	21
		S5	0	0	0	0	22	0	22
		S6	0	0	0	0	0	10	10
	%	S1	100.0	0.0	0.0	0.0	0.0	0.0	100.0
		S2	0.0	100.0	0.0	0.0	0.0	0.0	100.0
		S3	0.0	5.3	94.7	0.0	0.0	0.0	100.0
		S4	0.0	0.0	0.0	95.2	4.8	0.0	100.0
		S5	0.0	0.0	0.0	0.0	100.0	0.0	100.0
		S6	0.0	0.0	0.0	0.0	0.0	100.0	100.0

a. 98.1 % of original grouped cases correctly classified.

Table. 4. Structure matrix

Structure matrix

Variables	Function				
	1	2	3	4	5
% Sand	**.878***	-.284	.104	-.031	.258
MGS[b]	.492	-.462	-.353	.057	-.116
Sorting	**.474***	-.353	-.220	.138	-.096
Fe	.082	**.674***	-.593	.120	-.065
Ti[b]	-.025	.557	-.548	.079	-.126
Mn	.023	**.526***	-.212	-.105	.085
Ba[b]	.016	.467	-.419	.093	-.005
Red[b]	.032	-.431	.169	.013	-.030
Ca[b]	.041	-.284	.122	.147	.054
GL[b]	.035	-.256	-.010	-.070	-.013
% Clay	-.327	.500	**.585***	.479	.176
Blue[b]	-.047	-.316	.541	-.019	-.014
Green[b]	.020	-.379	.524	.024	-.029
MS	.083	.340	-.244	**-,549***	.461
% Silt	-.165	.511	.460	-.001	**-.536***

Pooled within-groups correlations between discriminating variables and standardized canonical discriminant functions. Variables ordered by absolute size of correlation within function.

*. Significant correlation between each variable and every discriminant function.

b. This variable not used in the analysis.

Table 5. PCA results

PCA results

Components	Eigenvalues	Explained variance (%)	Accumulated variance (%)
1	6.83	48.78	48.78
2	3.70	26.44	75.22
3	0.96	6.87	82.08
4	0.70	4.98	87.07

Components loading

	Component 1	Component 2	Component 3	Component 4
% Clay	-.430	**.852***	-.160	.079
% Silt	-.176	**.853***	-.174	.165
% Sand	.513	**-.744***	.260	.075
Sorting	.501	**-.790***	.203	.075
Fe	**.884***	.315	-.130	.184
Ti	**.895***	.199	-.016	.314
Ba	**.787***	.309	.267	.220
Mn	**.643***	.528	.310	.035
Ca	-.664	-.288	.079	**.642***
GL	.082	**-.618***	**-.706***	.161
MS (10^{-5} SI)	**.789***	.044	-.183	.041
Red	**-.804***	-.278	-.002	.114
Green	**-.942***	.055	.198	.104
Blue	**-.939***	.100	.186	.087

106 samples used in the analysis

* Significant variable ($p < 0.001$) for every component

Table. 6. Mean values of variables for each facies

Facies	Car-lok silt-clay facies		Car-lok sand facies		Fe-Ti sand facies	
Subfacies	S1	S2	S3	S4	S5	S6
Variables	Mean	Mean	Mean	Mean	Mean	Mean
Clay (%)	63.89	43.15	21.98	5.77	10.48	19.47
Silt (%)	35.85	46.72	24.94	13.27	19.37	30.24
Sand (%)	0.25	10.13	53.08	80.97	70.15	50.29
MGS (μm)	8.60	20.81	82.60	190.65	120.91	82.03
Sorting (μm)	12.12	24.86	71.03	125.27	86.38	71.34
Fe (p.a.)	12,891.33	13,367.84	11,835.36	11,920.71	19,800.91	50,959.20
Ti (p.a.)	213.88	279.69	252.76	242.37	435.86	1,303.41
Ba (p.a.)	34.71	39.18	31.83	36.77	48.29	97.52
Mn (p.a.)	188.57	247.65	163.23	123.48	256.76	547.69
Ca (p.a.)	166,495.64	178,198.01	189,383.77	185,141.13	129,951.01	115,241.88
GL	33,502.90	33,550.34	33,506.21	33,654.56	33,579.39	33,534.10
MS (10^{-5} SI)	2.63	4.74	3.01	2.90	12.41	17.02
Red	237.49	234.95	237.28	235.87	227.09	202.05
Green	227.22	221.85	223.76	206.97	190.71	170.56
Blue	203.78	193.27	196.22	165.04	137.43	107.71

106 samples used in the analysis. MGS= Mean Grain Size, GL = Grey Level and MS = Magnetic Susceptibility.

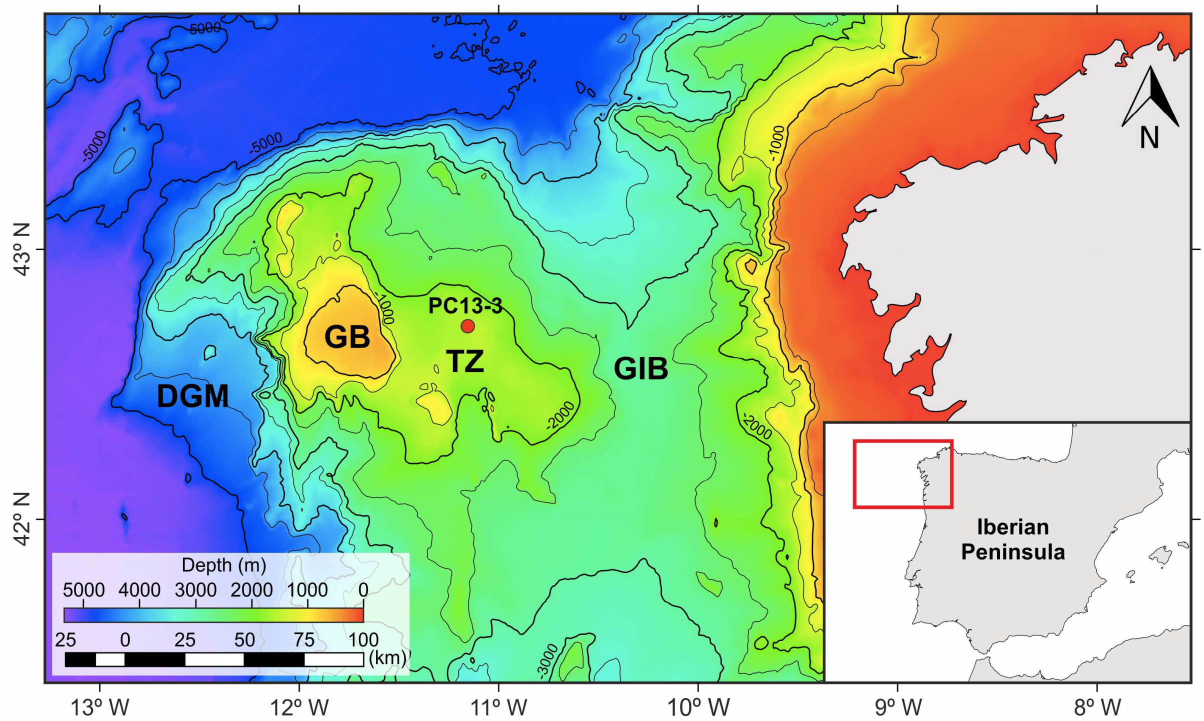

GB
TZ
GIB
DGM
PC13-3
N
Iberian Peninsula
Depth (m)
5000 4000 3000 2000 1000 0
25 0 25 50 75 100 (km)
-5000
5000
-1000
-2000
-3000
1000
43º N
42º N
13º W
12º W
11º W
10º W
9º W
8º W

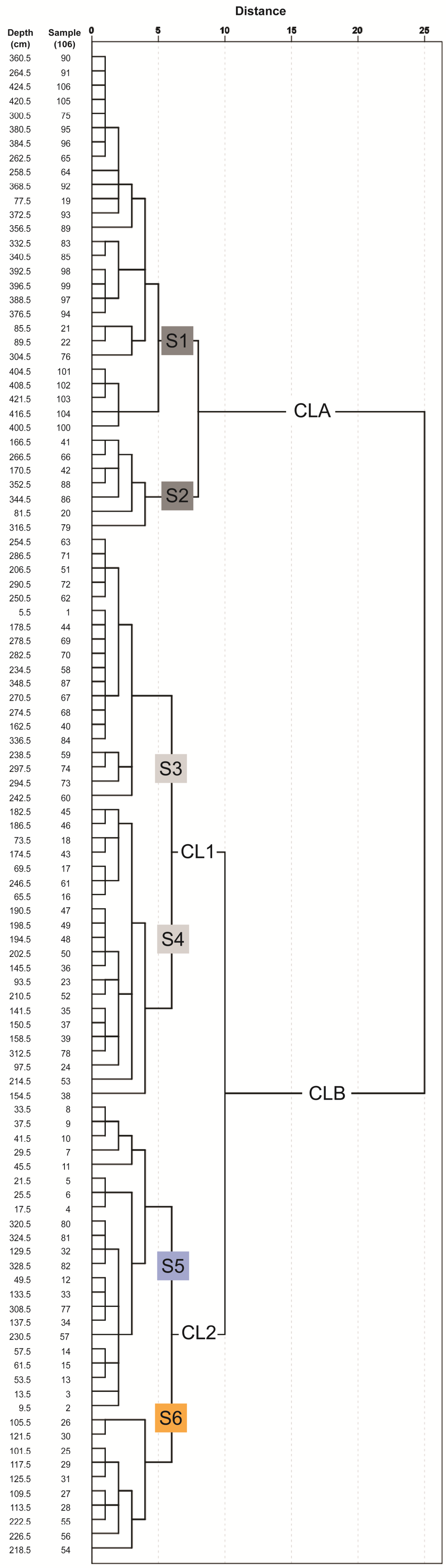

Distance
0
5
10
15
20
25
Depth (cm)
Sample (106)
360.5 90
264.5 91
424.5 106
420.5 105
300.5 75
380.5 95
384.5 96
262.5 65
258.5 64
368.5 92
77.5 19
372.5 93
356.5 89
332.5 83
340.5 85
392.5 98
396.5 99
388.5 97
376.5 94
85.5 21
89.5 22
304.5 76
404.5 101
408.5 102
421.5 103
416.5 104
400.5 100
166.5 41
266.5 66
170.5 42
352.5 88
344.5 86
81.5 20
316.5 79
254.5 63
286.5 71
206.5 51
290.5 72
250.5 62
5.5 1
178.5 44
278.5 69
282.5 70
234.5 58
348.5 87
270.5 67
274.5 68
162.5 40
336.5 84
238.5 59
297.5 74
294.5 73
242.5 60
182.5 45
186.5 46
73.5 18
174.5 43
69.5 17
246.5 61
65.5 16
190.5 47
198.5 49
194.5 48
202.5 50
145.5 36
93.5 23
210.5 52
141.5 35
150.5 37
158.5 39
312.5 78
97.5 24
214.5 53
154.5 38
33.5 8
37.5 9
41.5 10
29.5 7
45.5 11
21.5 5
25.5 6
17.5 4
320.5 80
324.5 81
129.5 32
328.5 82
49.5 12
133.5 33
308.5 77
137.5 34
230.5 57
57.5 14
61.5 15
53.5 13
13.5 3
9.5 2
105.5 26
121.5 30
101.5 25
117.5 29
125.5 31
109.5 27
113.5 28
222.5 55
226.5 56
218.5 54
S1
S2
CLA
S3
CL1
S4
CLB
S5
CL2
S6

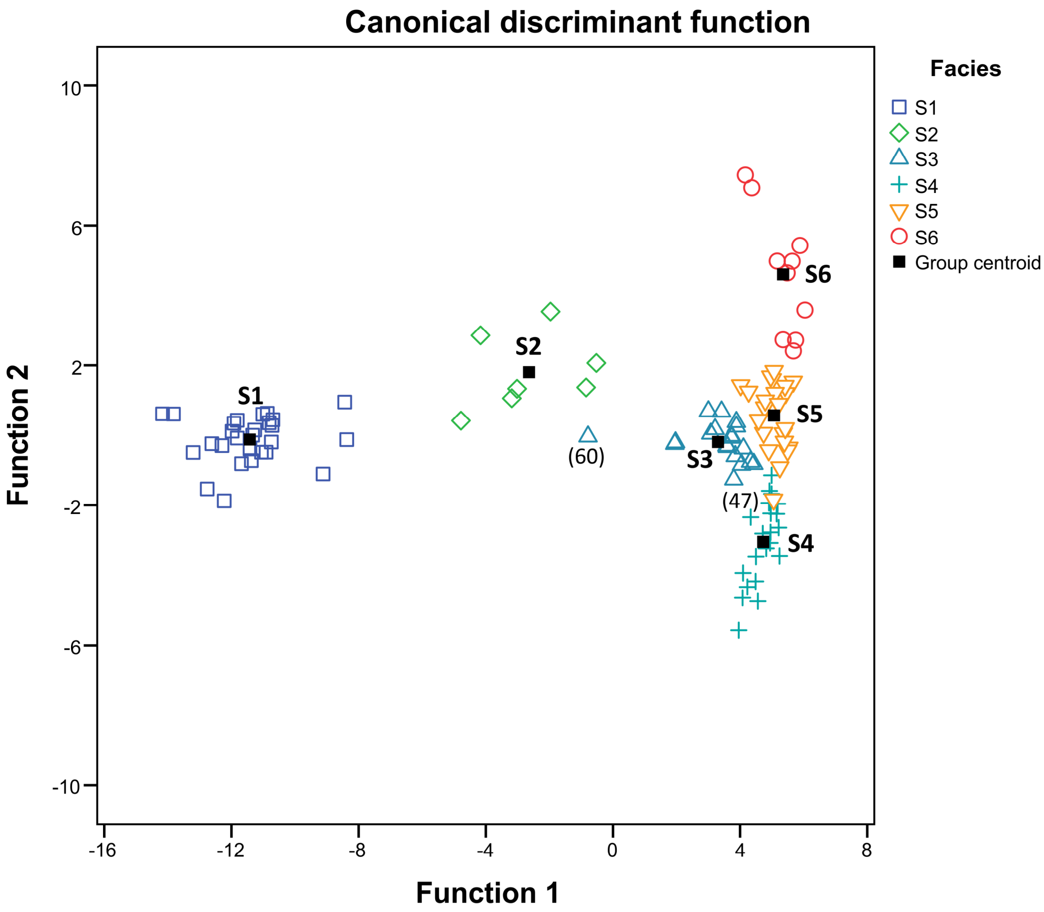
Canonical discriminant function
Facies
S1
S2
S3
S4
S5
S6
Group centroid
S1
S2
S3
S4
S5
S6
(60)
(47)
Function 2
Function 1
10
6
2
-2
-6
-10
-16
-12
-8
-4
0
4
8

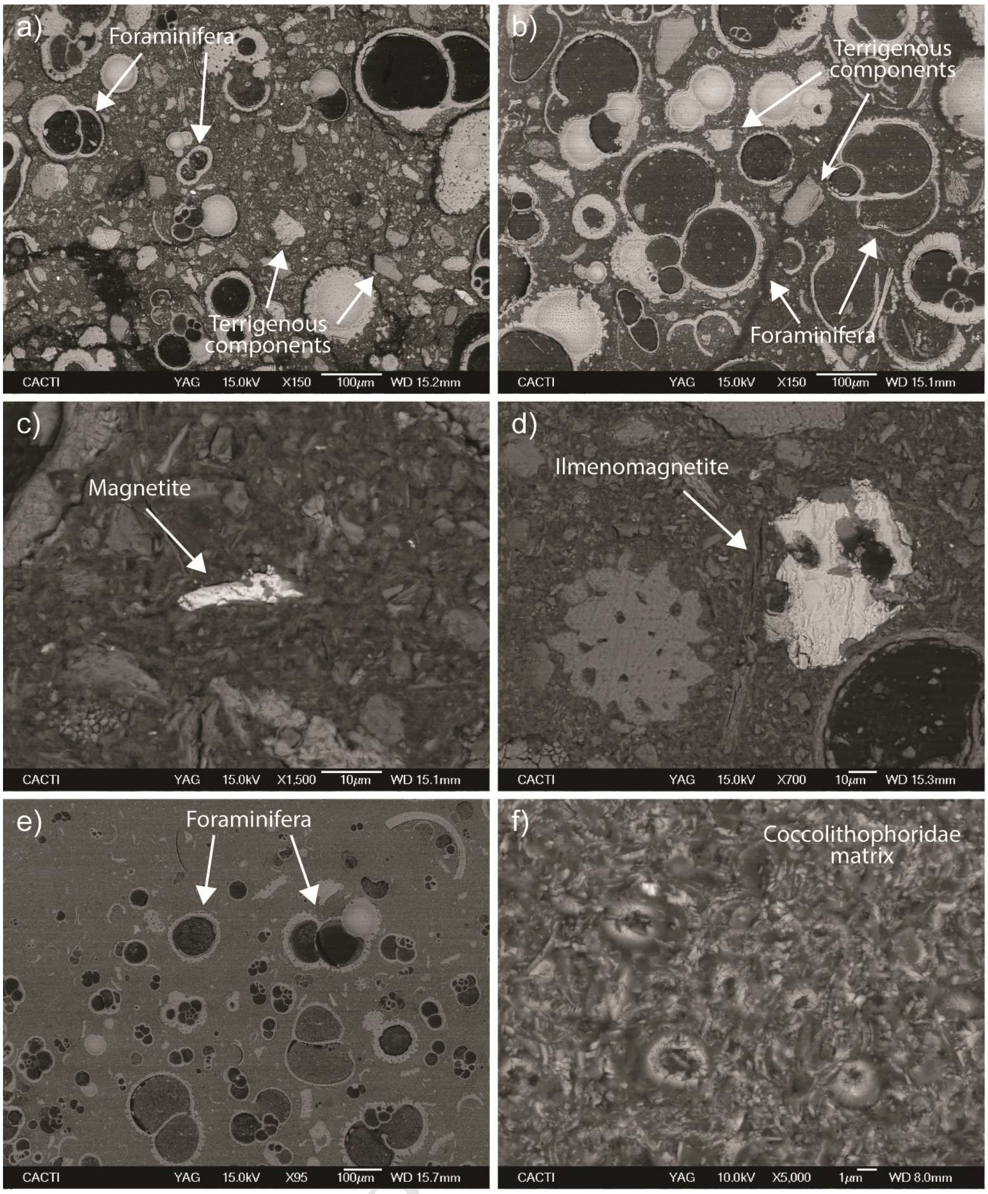
a)
Foraminifera
Terrigenous components
CACTI YAG 15.0kV X150 100μm WD 15.2mm
b)
Terrigenous components
Foraminifera
CACTI YAG 15.0kV X150 100μm WD 15.1mm
c)
Magnetite
CACTI YAG 15.0kV X1,500 10μm WD 15.1mm
d)
Ilmenomagnetite
CACTI YAG 15.0kV X700 10μm WD 15.3mm
e)
Foraminifera
CACTI YAG 15.0kV X95 100μm WD 15.7mm
f)
Coccolithophoridae matrix
CACTI YAG 10.0kV X5,000 1μm WD 8.0mm

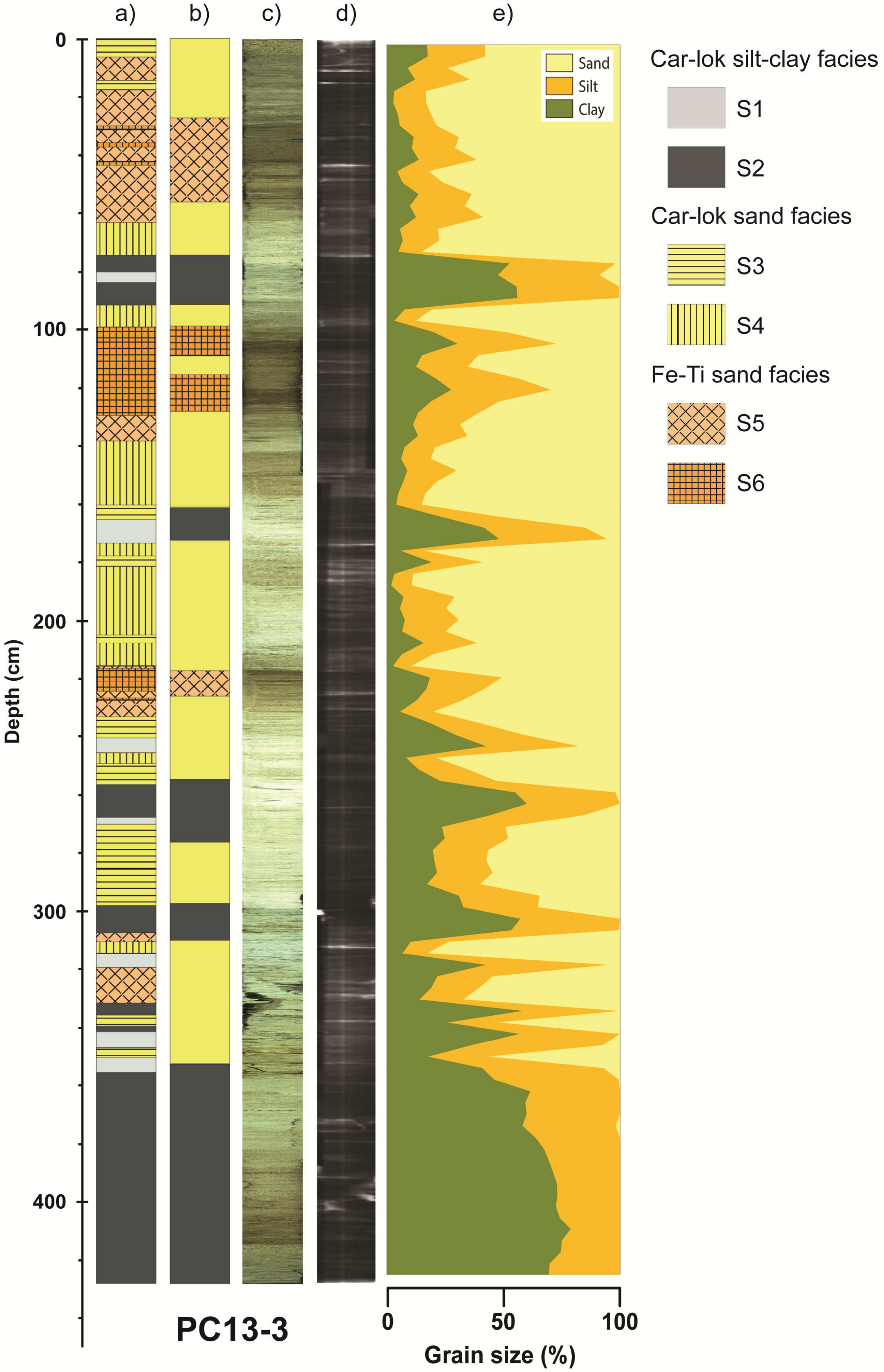
a)
b)
c)
d)
e)
Depth (cm)
0
100
200
300
400
Sand
Silt
Clay
Car-lok silt-clay facies
S1
S2
Car-lok sand facies
S3
S4
Fe-Ti sand facies
S5
S6
PC13-3
0
50
100
Grain size (%)